

Received 19 September 2023, accepted 19 November 2023, date of publication 27 November 2023, date of current version 1 December 2023.

Digital Object Identifier 10.1109/ACCESS.2023.3337030

## RESEARCH ARTICLE

# Optimal PEV Charging and Discharging Algorithms to Reduce Operational Cost of Microgrid Using Adaptive Rolling Horizon Framework

PHI-HAI TRINH<sup>1</sup>, (Student Member, IEEE), REHMAN ZAFAR<sup>1</sup>, (Student Member, IEEE), AND IL-YOP CHUNG<sup>1</sup>, (Member, IEEE)

Department of Electrical Engineering, Kookmin University, Seoul 02707, Republic of Korea

Corresponding author: Il-Yop Chung (chung@kookmin.kac.kr)

This work was supported in part by the Ministry of Science and Information and Communications Technology (MSIT), South Korea, under the Information Technology Research Center (ITRC) support Program Supervised by the Institute for Information and Communications Technology Planning and Evaluation (IITP) under Grant RS-2023-00259004; and in part by the Korea Institute of Energy Technology Evaluation and Planning (KETEP) grant funded by the Korean Government [Ministry of Trade, Industry and Energy (MOTIE)] under Grant 2022550000110.

**ABSTRACT** This paper presents an optimal operation algorithm for a grid-connected microgrid that incorporates renewable energy sources (RESs), plug-in electric vehicle (PEV) charging/discharging stations, and local loads. The aim of this work is to not only propose a microgrid operating algorithm but also implement it within the microgrid energy management system. The primary objective of the proposed algorithm is to reduce the overall operational cost of the microgrid while minimizing the PEV charging bills simultaneously. To this end, we propose an adaptive PEV power charging/discharging and power exchange (grid exporting/importing) scheduling strategy that accounts for the uncertainty of RES power generation, loads, and electric pricing. To address the dynamic arrival of PEVs, we propose an online optimization scheme using an adaptive rolling horizon framework. The size of the rolling window is adjusted in each time step to adapt to the dynamic nature of the PEV charging period. Additionally, we propose the design of a dynamic pricing model for PEV charging and discharging to achieve power system balance within the microgrid, thereby optimizing operating costs and minimizing PEV charging bills further. Through simulations, we demonstrate the effectiveness of the proposed strategies, which are expected to benefit both the microgrid operators and PEV owners.

**INDEX TERMS** Adaptive rolling horizon framework, dynamic pricing, plug-in electric vehicle charging/discharging, microgrid optimal operation, operating cost.

## NOMENCLATURE AND ACRONYMS

### A. ACRONYMS

*DER* Distributed energy resource.  
*PEV* Plu-in electric vehicle.  
*EVCS* Electric vehicle charging station.  
*ARH* Adaptive rolling horizon.

*LSTM-RNN* Recurrent-neural-network-based long short-term memory.  
*MG-EMS* Microgrid energy management system.  
*MILP* Mixed-integer linear programming.  
*MILCQP* Mixed integer linear constrained quadratic programming.  
*PV* Photovoltaic.  
*RES* Renewable energy source.  
*SMP* System margin price.  
*SoC* State of charge of the PEV battery.  
*ToU* Time of use.  
*V2G* Vehicle to grid.

The associate editor coordinating the review of this manuscript and approving it for publication was Shafi K. Khadem.

**B. PARAMETERS**

$\varphi_{ch}^i$	Proposed charging price of the PEV at the $i$ -th interval.
$\varphi_{disch}^i$	Proposed discharging price of the PEV at the $i$ -th interval.
$E_{cap}^m$	Capacity of $m$ -th connected PEV.
$N_{EV}^i$	Number of PEVs connected at the $i$ -th interval.
$N_{connect}^{m,i}$	Size of the connection period of $m$ -th PEV at the $i$ -th interval.
$P_{c,max}^m, P_{d,max}^m$	Maximum charging/discharging power of the $m$ -th EVCS.
$P_{g,max}^b, P_{g,max}^s$	Maximum power import/export from/to the utility grid.
$P_{NL}^i$	Total netload at the $i$ -th interval.
$P_L^i, P_{PV}^i$	Total load consumption and PV power generation at the $i$ -th interval.
$P_{cri}$	Maximum power import to the microgrid without causing peak-demand charge defined as critical power.
$SoC^{m,i}$	SoC of the $m$ -th PEV at the $i$ -th interval.
$SoC_{request}^m$	SoC request for the $m$ -th PEV.
$SoC_{max}^m, SoC_{min}^m$	Maximum/minimum SoCs of the $m$ -th PEV.
$T_{connect}^{m,i}$	Connection period of the $m$ -th PEV at the $i$ -th interval.
$T_{ARH}^i$	ARH period at the $i$ -th interval.
$W_{ARH}^i$	Size of the ARH at the $i$ -th interval.
$W_{FRH}^i$	Size of the fixed rolling horizon at the $i$ -th interval.
$\phi_{obj}^i$	Objective function at the $i$ -th interval.
$\phi_{NEC}^i, \phi_{PDC}^i$	Total cost for net energy cost and peak-demand charge at the $i$ -th interval.
$\varphi_{PDC}$	Peak-demand charge price.
$\varphi_{ToU}^i, \varphi_{SMP}^i$	ToU price and SMP at the $i$ -th interval.
$\delta^{m,j}$	State of connection of the $m$ -th PEV at the $j$ -th interval.
$\beta$	Penalty for PEV charging at the peak-demand period.
$\gamma$	Incentive for PEV discharging at the peak-demand period.
$\eta_c^m, \eta_d^m$	Charging and discharging efficiencies of the $m$ -th connected PEV.

**C. VARIABLES**

$s_c^{m,j}, s_d^{m,j}$	Charging and discharging rates of the $m$ -th PEV at the $j$ -th interval.
$P_g^{b,j}, P_g^{s,j}$	Electric power purchased/sold from/to the grid at the $j$ -th interval.
$\kappa^{m,j}$	Charging/discharging state of the $m$ -th PEV at the $j$ -th interval.
$\mu_g^j$	Import/export state of power at the $j$ -th interval.

**I. INTRODUCTION**

The concept of microgrid has been proposed to improve the local reliability and flexibility of electric power system and is defined as a group of controllable DERs, loads, and energy storage units [1]. The idea supporting the formation of the microgrid involves a paradigm consisting of a cluster of distributed generations and aggregated loads that is adequately reliable and economically viable as an operational electric system [2], [3]. A microgrid combined with RESs is a preferred solution to the escalating energy crisis as well as environmental concerns [4]. In the presence of RESs, microgrid management is a challenging task. Mostly, MG-EMSs have been widely utilized to manage microgrids. The microgrid central controller makes bids for energy supply and ancillary services to the electricity market based on the forecast market prices, renewable power output, and load. Day-ahead power consumption and generation scheduling are performed according to the collected information on market prices, power forecasts, and status of the units. In this manner, MG-EMSs settle the bids for energy and ancillary services, setpoints of the controllable distributed generators (DGs), charging/discharging states of the energy storage systems, and control of the loads. Moreover, the dispatch and bidding strategies in the controller should maximize the total financial income of the microgrid, including its revenue from the electricity market and local consumers after subtracting the operational cost of the generating unit and payback cost of load curtailment [5].

Nowadays, many countries are promoting low-energy or zero-energy buildings, in which the buildings can meet their energy demands economically and in an environmentally friendly manner through locally available generation and RESs. They have also promoted the development of DC loads, such as LED lighting, battery energy storage systems (BESSs), and plug-in electric vehicles (PEVs). Corresponding to these changes, many studies have indicated that DC microgrids are suitable for the distribution systems in buildings. DC microgrids are the most efficient method of using DC electricity from onsite power generation, such as PV, fuel cells (FCs), and BESSs [6]. The consumer equipment today and DG units of tomorrow are dominated by power electronic devices. In [7], the authors compared the advantages of DC microgrids over AC microgrids in terms of conversion efficiency, cost of the converters, transmission efficiency, power supply reliability, controllability, load availability, and protection. On the other hand, PEV integration would be more efficient with the DC system, which is another important component of a microgrid in the near future. The widespread deployment of PEVs is expected to be a solution to the global shortage of fossil fuels as well as air pollution crisis [8], [9]. The emission reduction goal is achieved by appropriate and optimal utilization of PEVs as energy storage systems and loads in a power system integrated with RESs [10], [11], [12].

There are various studies on PEV integration with microgrids and optimal PEV charging/discharging algorithms to

**TABLE 1.** Comparison of the proposed work with other methods.

Reference	Objective Model	Solution method	EV Uncertainties	PV/Load uncertainties	Peak-load reduction
[22]	Optimally manage a microgrid.	MILP, RH	No	Yes	No
[23]	Minimize the risk of uncertainty of load demand, PV, WT and electricity price.	MILCQP, RH	No	Yes	No
[24]	Maximize economic benefit for the prosumers.	MILP	Yes	Yes	No
[25]	Maximize benefit of the aggregator	Two-stage robust optimization, RH	No	Yes	Yes
Proposed work	Minimize operating cost of MG and EV charging cost	MILP, ARH	Yes	Yes	Yes

improve the economic advantages from PEV interconnection. In [13], the event-driven model predictive control (MPC) approach is used to perform cost-effective charging operations for PEVs considering user preferences as well as various grid and PEV constraints. The optimal management model for a smart house with a vehicle-to-grid (V2G) system was presented in [14]; this system was considered as a residential microgrid that consists of RESs, house load, and PEV charging point for V2G services. In [15], a two-stage economical operation of a microgrid-like PEV parking deck system was proposed; this system comprised PV panels and PEVs as the DERs and charging loads. The MPC-based online control strategy was used for PEV charging while reducing the forecast errors of PEV parking behaviors to increase the revenue of the parking deck. In [16], a power dispatch scheme was presented for the DERs in a distributed system by considering PEV uncertainties based on the MPC approach; the PEV was used as a charging load in this system, and the MPC-based online power dispatch method was used to mitigate PEV uncertainty on the basis of PEV information, such as number of PEVs connected to the charging stations, battery capacity, SoC, and arrival and departure times. The objective of this system was to minimize the operational cost. The smart charging mechanism of a PEV using a PV system in the microgrid was proposed in [17]; the system contained five components, namely energy management system, controllable load, uncontrollable load, PV panels, and PEVs. This microgrid works in an interconnected mode of operation, and an optimization algorithm using predictions for the PV and load demand as well as V2G with linear programming was used to solve the problem; the objective of the study was to increase the consumption of PV power and decrease the peak demand. In [18], authors analyzed PEV power consumption during peak and valley times and proposed a novel stochastic unit commitment algorithm for optimal PEV charging considering renewable energy integration.

The connection of PEVs to power grids pose many technical challenges that need to be addressed. With the widespread adoption of PEVs, power systems may face significant challenges owing to the large electricity demands of these loads. Moreover, microgrids are impacted by the growing penetration of PEVs, which represents a new dimension for

microgrid management, where large amounts of energy storage will be injected to the grid through millions of PEVs [19]. The major technical challenges in microgrid control and operation are the dynamic arrival of PEVs and uncertainties in the load and PV generation. The arrival of PEVs is known to be an unpredictable component as it depends on the PEV owners' behaviors and electricity charging prices, whereas PV power generation and load consumption are known to be time-varying uncertainty components that depend on the weather conditions and consumer behaviors, respectively. There have been several researches to consider the uncertainties in PEVs. Authors in [20] and [21] addressed PEV uncertainties with a decentralized fuzzy data fusion approach. They optimized charging station management with fuzzy integer linear programming and minimized EV waiting times using a fuzzy inference system.

In this paper, to address the dynamic arrival of PEVs and uncertainties in load and PV supply, we propose a novel microgrid operation strategy that enables the overall operation to be more efficient and effective. The uncertainties are considered in the optimization using deep-learning based forecasting algorithms and model predictive control with adaptive rolling horizon (ARH) framework. Forecasts can be updated regularly with new information and integrated into rolling horizon optimization framework. This allows the system to adapt to various operating conditions and make optimal decisions based on the most recent available data. On the other hand, the employment of ARH framework is also to determine the number of connected PEVs at each time step so that the PEV information including arrival time, departure time, initial SoC, departure SoC and ARH window are updated at each time step and take into account in the optimization process. Therefore, the optimization method combined with the ARH framework that can adapt to unpredictable PEV arrivals, load and PV uncertainties and fragile grid-related constraints. The main objective of this work is to minimize the total cost of microgrid operation, including minimization of the peak-demand charge, PV curtailment reduction, load consumption, and charging/discharging of the PEVs.

Table 1 shows a comparison of our main contribution with another researches. The main contributions of this work are as follows.

- 1) We propose a multistep optimization scheme using the ARH framework. We formulate the local scheduling optimization problem using mixed-integer linear programming (MILP), which aims to minimize the total operating cost of the microgrid as well as enhance customer satisfaction.
- 2) We propose a retail dynamic electricity price for PEV charging and discharging based on local load consumption and PV power generation. The pricing model can maximize the benefits of both the microgrid operators and PEV customers.
- 3) Based on the proposed dynamic pricing model, we also propose a control strategy for PEV charging and discharging to maximize the PV power production using the ARH framework. At the peak power generation period, the PEV owners are encouraged to charge their PEV batteries by providing them competitively low charging prices so as to reduce PV power curtailment. Furthermore, the PEVs are set to be discharged at the peak demand intervals to maintain the loads at the critical power.

The remainder of this paper is organized as follows. Section II describes the problem formulation, including the system background, objective function, proposed ARH framework, and dynamic pricing model. Section III presents the results and discussion of this work. Section IV presents the conclusions drawn from the findings in this work.

## II. METHODOLOGY

In this section, the overall methodology of the proposed approach is discussed. First, the system description is provided to understand the system scale and assumptions. Then, the control strategy is described along with the mathematical problem formulation.

### A. SYSTEM DESCRIPTION

The proposed microgrid used in this work consists of one main AC/DC converter interconnected to a 22.9 kV medium-voltage AC grid in the grid-connected mode and a PV generation system located on the rooftop of a building. All entities are connected to the DC microgrid via power electronic devices. There is multiple plug-in EVCSs and PEV fast-charging stations installed near the building and connected to the DC microgrid system, as shown in Fig. 1. The charging and discharging actions of all EVCS are managed by the microgrid operator. The electrical load and PV generation profiles are obtained from the advanced forecasting model using a recurrent neural network (RNN)-based long short-term memory (LSTM) algorithm. The arrival of PEVs for charging and discharging are created based on randomly selected cases.

Fig. 1 illustrates the configuration of the MG-EMS that manages the load, sources, and EVCS to achieve potential objectives, such as energy balance, peak shaving, and PEV charging/discharging operations.

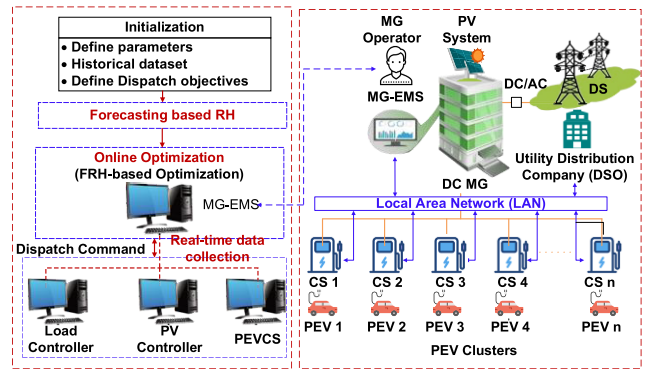


FIGURE 1. Microgrid and its EMS (MG-EMS).

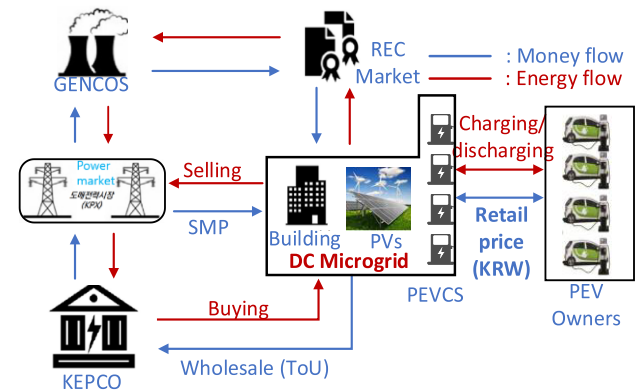


FIGURE 2. Energy exchange model of the microgrid with EVCS.

In this study, we assume that the microgrid operator is a mediator between the utility provider and end PEV customers; the operator procures electricity from the power distribution company and resells it to the PEV owners. In this work, we also assume that the microgrid is able to host RESs (i.e., solar power) and use the generated power or sell it back to the utility provider or PEV owners. An overview of the energy exchange model of the microgrid system is illustrated in Fig. 2.

### B. PROPOSED FRAMEWORK

The total operational cost is minimized based on the information concerning the loads, connected PEVs, PV generation, and electricity rates. The PV power generation and load consumption are known to be time-varying uncertainty components that depend on the weather conditions and consumer behaviors, respectively. To solve these problems, we apply an advanced forecasting algorithm for the load and PV power generation based on the LSTM-RNN to predict the load and PV requirements in a day-ahead sequence [26], [27].

Most studies use the day-ahead optimal scheduling scheme to provide the global minimized total cost [28], [29]. However, this approach is impractical as it requires information regarding the PEVs, loads, and PV profiles in the future (for example, the subsequent 24 hours). In particular, it is fairly

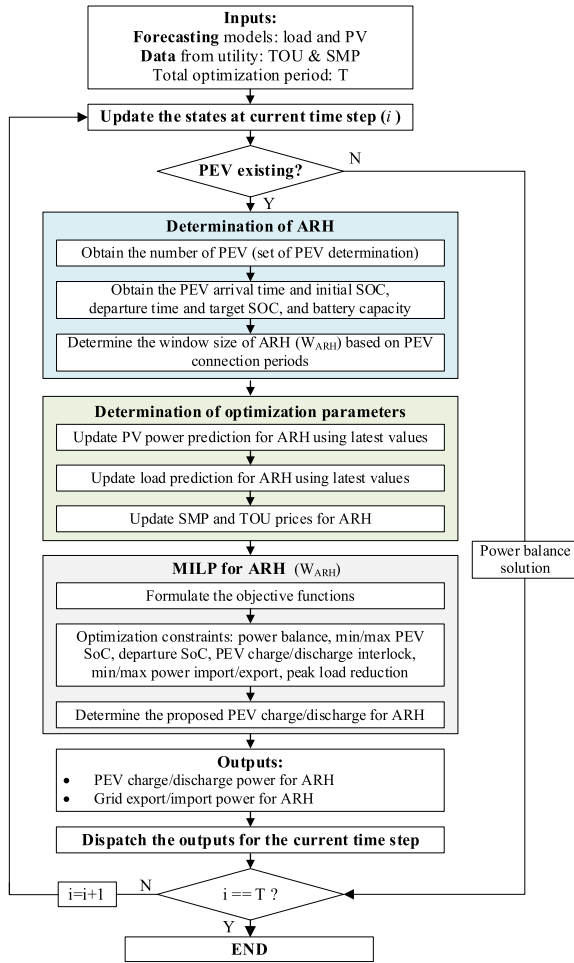


**FIGURE 3.** Flowchart of the adaptive rolling horizon (ARH) control strategy.

difficult to predict the arrival time and charging period of an PEV on a given day. Therefore, in this study, we apply the ARH scheme to optimize and schedule the operating cost within the adaptive moving window. Because we use the ARH framework, the proposed approach is more practical and useful for PEV charging and discharging systems, and the operator can easily and efficiently handle dynamic PEV arrivals.

Furthermore, the peak-demand charge and PV power curtailment are some of the most important problems for microgrid systems. Variations in the load, PV power generation, and PEV charging/discharging power can easily cause peak-demand charges. Hence, the proposed control strategy considering PEV charging and discharging can also minimize peak-demand charge and PV curtailment.

In this paper, we propose a rolling horizon strategy to enable the dynamic behavior of the microgrid system with the integration of PEVs. This rolling horizon approach is an iterative process that seeks to determine the optimal solution for the objective function within a time window at each time step, as illustrated in Fig. 3. The process consists of the following steps:

- *Step 1:* The first step is to obtain the inputs for the proposed method, such as the forecast values for the load and PV generation power, as well as electricity prices, such as SMP and ToU prices from the power utility company. The LSTM based RNN forecasting algorithms play a crucial role in the optimization problem. The accuracy of the forecasting algorithm affects to the decisions in real-time, leading to a cost-effective and reliable operation of the microgrid
- *Step 2:* We check whether there are any PEVs connected at the current time step. If there are PEVs connected, the ARH is determined using the number of PEVs connected and their durations of connection. In addition, the forecast values of PV power and load as well as dynamic pricing are determined for the ARH window size. If there are no PEVs connected at the current time step, the power balance is calculated, and the process moves to step 4 with an ARH window size of one-time step.
- *Step 3:* The MILP problem is formulated and solved for the ARH by taking into account the PEVs, grid, and other balancing constraints. The obtained solution consists of an PEV charging or discharging schedule and power export/import from the grid for the ARH. In this step, only the solution for the first-time step of the ARH is applied to the actual operation.
- *Step 4:* The process moves to step 2 with updated states and is repeated.

Through this rolling horizon approach, we can effectively manage the dynamic behavior of the microgrid system and minimize costs while maximizing efficiency. The problem is thus formulized with the objective function and constrains by considering various control variables.

*Objective function:* The total operating cost of the microgrid is determined by the total cost of net energy charge and peak-demand charge. Net energy and peak demand can be reduced by PV power generation or control of the charging and discharging of the PEVs. The optimization is executed for the ARH ( $W_{ARH}^i$ ) from the  $i$ -th time step that is governed by a set of objective functions. The mathematical formulations for the objective functions are described in (1)–(5), subject to the constraints (6)–(14)

$$\min \phi_{obj}^i \tag{1}$$

where  $\phi_{obj}^i$  is comprised of the cost function of net energy charge and peak-demand charge of the microgrid at the  $i$ -th interval.

$$\phi_{obj}^i = \phi_{NEC}^i + \phi_{PDC}^i \tag{2}$$

The net energy charge of the microgrid is defined as:

$$\begin{aligned} \phi_{NEC}^i &= \sum_{j=i}^{i+W_{ARH}^i} \left[ \sum_{m=1}^{N_{PEV}^j} \left( \varphi_{ch}^j \delta^{m,j} s_c^{m,j} P_{c,max}^m + \varphi_{disch}^j \delta^{m,j} s_d^{m,j} P_{d,max}^m \right) \right] \end{aligned}$$

$$+ \varphi_{ToU}^j P_g^{b,j} - \varphi_{SMP}^j P_g^{s,j} \quad (3)$$

The cost function  $\phi_{NEC}$  aims to minimize the load consumption, which includes the PEV charging and discharging cost, grid power imports and maximize the grid power export to minimize the overall operating costs. The optimization window ( $W_{ARH}$ ) is determined at the beginning of the  $i$ -th time step based on the PEV information. The PEV charging and discharging costs ( $\varphi_{ch}^j, \varphi_{disch}^j$ ) within the ARH window are calculated using our proposed dynamic pricing model, as presented in section II-D. Other parameters such as the cost for grid export/import power ( $\varphi_{ToU}^j, \varphi_{SMP}^j$ ) are pre-defined by the utility.

The cost function  $\phi_{PDC}$  aims to minimize the peak-load demand charges by optimizing PEVs' charging and discharging. It takes into account the peak-demand charging price ( $\varphi_{PDC}$ ) to ensure that the peak-load remains below the critical power threshold ( $P_{cri}$ ). The critical power is determined by historical peak data or the contractual agreement with the utility company. The unit-step function, denoted as  $u(x)$ , is employed to adjust the peak-demand charges according to the net load power relative to the critical power. This approach effectively manages peak-loads and reduces the peak-demand charges.

$$\begin{aligned} \phi_{PDC}^i = & \sum_{j=i}^{i+W_{ARH}^i} \varphi_{PDC} \left[ u \left( P_{NL}^j - P_{cri} \right) \right. \\ & \left. \cdot \left( P_{NL}^j - P_{cri} + s_c^{m,j} P_{c,max}^m - s_d^{m,j} P_{d,max}^m \right) \right] \end{aligned} \quad (4)$$

$$u \left( P_{NL}^j - P_{cri} \right) = \begin{cases} 1, & P_{NL}^j - P_{cri} > 0 \\ 0, & P_{NL}^j - P_{cri} \leq 0 \end{cases} \quad (5)$$

where  $j = i, \dots, i + W_{ARH}^i, m = 1, \dots, N_{EV}^i$

The aforementioned objective functions are expressed as the convex optimization problems and can be solved using an optimization solver such as CPLEX/MATLAB. However, it is necessary to establish a set of constraints to solve the optimization problem successfully. One of the most critical constraints is demand–supply balance that ensures that the microgrid operates smoothly by taking into account the local load demand, PV power generation, total charging and discharging PEV power, and power imported from and exported to the utility system. The power balance constraint at the  $j$ -th time step is as follows [31]

$$P_g^{b,j} + \sum_{m=1}^{N_{EV}^i} s_d^{m,j} P_{d,max}^m + P_{PV}^j = P_g^{s,j} + P_L^j + \sum_{m=1}^{N_{EV}^i} s_c^{m,j} P_{c,max}^m \quad (6)$$

where  $j = i, \dots, i + W_{ARH}^i, m = 1, \dots, N_{EV}^i$

To prevent overloading of the microgrid, it is essential to ensure that the total power drawn from the grid at any given time step does not exceed the corresponding maximum power

limit. Additionally, it is necessary to prohibit scenarios in which power is both exported to the grid and imported from the grid simultaneously in the microgrid.

$$P_g^{b,j} \leq \mu_g^j P_{g,max}^b \quad (7)$$

$$P_g^{s,j} \leq \left( 1 - \mu_g^j \right) P_{g,max}^s \quad (8)$$

$$\mu_g^j = \begin{cases} 1, & \text{import} \\ 0, & \text{export} \end{cases} \quad (9)$$

Similarly, the  $m$ -th connected PEV can charge, discharge, or remain idle at every  $j$ -th interval when connected to the microgrid. However, the charging and discharging power must not exceed the maximum power limited by the power converter. In addition, power exchange between PEVs should be banned, and the PEV discharging power must be used only for peak load reduction in the microgrid. The state of charge (SoC) of the PEV batteries should be restricted by upper and lower limits that are given by the battery manufacturer. Each PEV needs to be sufficiently charged to guarantee the minimum SoC requirements requested by the PEV owner for their next travel.

$$0 \leq s_c^{m,j} \leq \kappa^j \quad (10)$$

$$0 \leq s_d^{m,j} \leq \left( 1 - \kappa^j \right) \quad (11)$$

$$\kappa^j = \begin{cases} 1, & \text{when PEV charged} \\ 0, & \text{when PEV discharged} \end{cases} \quad (12)$$

$$SoC_{min}^m \leq SoC^{m,j} \leq SoC_{max}^m \quad (13)$$

$$SoC^{m,k} \geq SoC_{request}^m \quad (14)$$

where  $j = i, \dots, i + W_{ARH}^i, m = 1, \dots, N_{PEV}^i$ , and  $k$  is the departure time of the  $m$ -th PEV.

The SoC at each time step can be obtained by considering the initial SoC and charging or discharging of the PEV battery. The SoC of the  $m$ -th connected PEV at time step  $j$ , denoted as  $SoC^{m,j}$ , is given by

$$\begin{aligned} SoC^{m,j} = & SoC^{m,h} \\ & + \sum_{i=h+1}^j \left( \frac{\eta_c^m s_c^{m,i} P_{c,max}^m T_s}{E_{cap}^m} - \frac{s_d^{m,i} P_{d,max}^m T_s}{\eta_d^m E_m^{cap}} \right) \end{aligned} \quad (15)$$

where  $SoC^{m,h}$  represents the initial SoC of the connected PEV  $m$ -th,  $\eta_c^m, \eta_d^m$  are the charging and discharging efficiencies of the  $m$ -th connected PEV, respectively.  $T_s$  is the given sampling time

The objective function outlined above calls for implementation of an ARH approach at each interval denoted by  $i$ . This is paired with a time-varying model for PEV charging/discharging that belongs to an adaptive window. The following subsections delve into further details regarding the proposed ARH and dynamic pricing model.

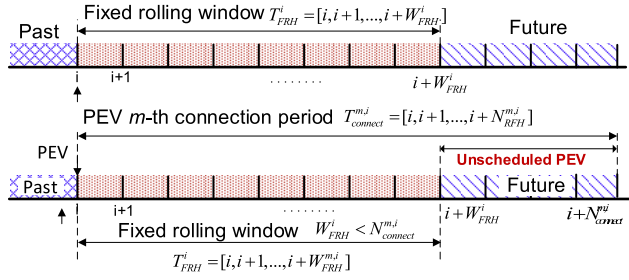


FIGURE 4. Conventional rolling horizon framework for microgrid operation.

**C. ARH FRAMEWORK FOR MICROGRID OPTIMIZATION CONSIDERING DYNAMIC PEV ARRIVALS**

There are several studies on the rolling horizon framework for online optimization problems in microgrid operation [32]. According to extant studies, the rolling window horizon is set for fixed time steps ( $W_{FRH}$ ) without considering temporal integration of the PEV with other DERs. In this case, the system can be easily updated for system states, such as PV forecasting, load forecasting, and PEV, with a few shortcomings. For example, if the window size for the connection period ( $N_{connect}^{m,i}$ ) of the  $m$ -th PEV is larger than that of the fixed rolling horizon (FRH) window ( $W_{FRH}^i$ ), the system is unable to attain optimal scheduling results over the rolling horizon owing to the inability to fully utilize the PEV while it is connected to the EVCS, as shown in Fig. 4. Furthermore, if the window size of the connection period of the  $m$ -th PEV is less than that of the FRH window ( $N_{connect}^{m,i} < W_{FRH}^i$ ), the number of variables in the optimization problem increases unnecessarily, thus increasing the computational burden.

In this paper, we present the ARH framework by considering the dynamic arrival of the PEV. The ARH is the rolling horizon framework with a flexible sliding window size that can adapt to the changes in PEVs connection period. The size of the adaptive rolling window ( $W_{ARH}^i$ ) is adaptively changed in each time step based on the longest connection period of the PEVs connected to the EVCS. The size of the ARH determination can be decomposed into the following steps:

- *Step 1:* At the current time step  $t = i$ , the system operator acquires the PEV information regarding PEV availability, number of PEVs connected to EVCS, and their arrival and departure times. The connection period of the  $m$ -th PEV at the current time  $i$  is subsequently obtained as

$$T_{connect}^{m,i} = [i, i + 1, \dots, i + N_{connect}^{m,i}], \quad m = 1, \dots, N_{EV}^i \quad (16)$$

The size of the connection period for the  $m$ -th PEV at the current time step  $i$  ( $N_{connect}^{m,i}$ ) is defined as the length of the PEV connection period.

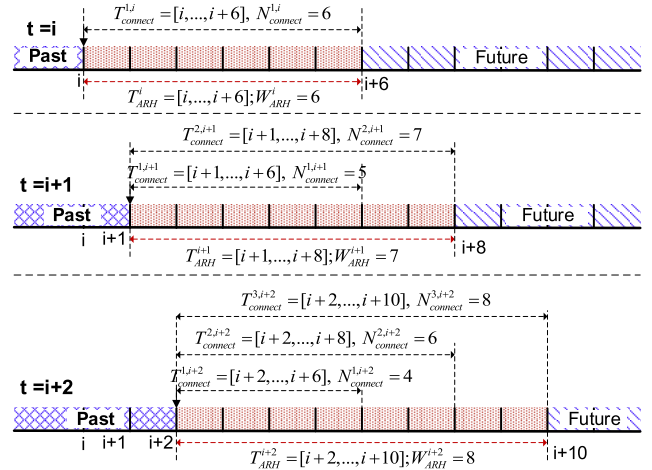


FIGURE 5. Adaptive rolling horizon framework for MG microgrid operation.

Based on the connection period of the PEV, the ARH period is determined as

$$T_{ARH}^i = [i, i + 1, \dots, i + W_{ARH}^i] \quad (17)$$

The ARH size ( $W_{ARH}^i$ ) at the current time step  $i$  is determined by choosing the maximum among the window sizes of the connection periods of the connected PEVs.

$$W_{ARH}^i = \max [N_{connect}^{1,i}, N_{connect}^{2,i}, \dots, N_{connect}^{m,i}] \quad (18)$$

In the case that no PEV is participating during the  $i$ -th time step, the ARH size is set to a single time step as

$$T_{FRH}^i = [i, i + 1], \quad W_{ARH}^i = 1 \quad (19)$$

- *Step 2:* At the current time step  $t = i + 1$ , it is necessary to update all PEV information to accurately reflect the current state of the system. This process involves repeating step 1, which entails determination of the ARH size at the current time step ( $i + 1$ ) ( $W_{ARH}^{i+1}$ ). By continuously updating the PEV information and recalculating the ARH at each time step, the system is able to adapt and optimize the overall cost in response to changing system states.

The process of the ARH is intuitively described here. At the current time step  $i$ , the system operator determines one connected PEV at the EVCS with the connection period as.

$$T_{connect}^{1,i} = [i, i + 1, \dots, i + N_{connect}^{1,i}] \quad \text{where } N_{connect}^{1,i} = 6.$$

The ARH period is then described as

$$T_{ARH}^i = [i, i + 1, \dots, i + W_{ARH}^i] \quad \text{where } W_{ARH}^i = N_{connect}^{1,i} = 6$$

At the current time step ( $i + 1$ ), the new PEV is connected to the system, and the connection periods are updated as

$$T_{connect}^{1,i+1} = [i + 1, i + 2, \dots, i + 1 + N_{connect}^{1,i+1}]$$

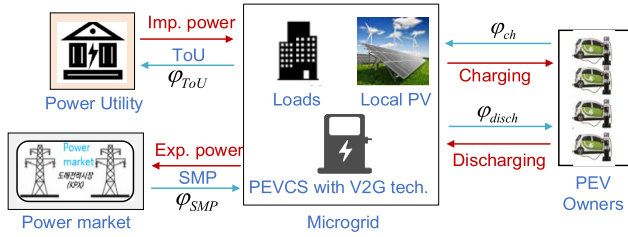


FIGURE 6. Proposed dynamic pricing model for PEV customers.

$$\begin{aligned} & \text{where } N_{connect}^{1,i+1} = 5 \\ T_{connect}^{2,i+1} &= [i + 1, i + 2, \dots, i + 1 + N_{connect}^{2,i+1}] \\ & \text{where } N_{connect}^{1,i+2} = 7 \end{aligned}$$

The ARH period is then determined as

$$T_{ARH}^{i+1} = [i + 1, i + 2, \dots, i + 1 + W_{ARH}^{i+1}]$$

where  $W_{ARH}^{i+1} = \max [N_{connect}^{1,i+1}, N_{connect}^{2,i+1}] = 7$

Similarly, we can easily determine the ARH period at the current time step ( $i + 2$ ) based on the updated connection periods of PEVs 1, 2, and 3.

$$T_{ARH}^{i+2} = [i + 2, i + 3, \dots, i + 2 + W_{ARH}^{i+2}]$$

where  $W_{ARH}^{i+2} = \max [N_{connect}^{1,i+2}, N_{connect}^{2,i+2}, N_{connect}^{3,i+2}] = 8$

We can easily see that the ARH changes to adapt to the dynamic arrival of PEVs from five intervals at the  $i$ -th time step to seven intervals at the  $(i + 1)$ -th time step and up to eight intervals at the  $(i + 2)$ -th time step. Therefore, all PEVs are involved in the optimization process. Fig. 5 shows an example of determination of the ARH.

### D. PROPOSED ELECTRICITY PRICING MODEL FOR PEVS

Currently, the electricity pricing mechanism includes the catalog price, stepwise power tariff (SPT), time-of-use (ToU), and real-time price [33], [34], [35]. The ToU price, which is the most popular pricing model in recent years, has different prices for different time periods in a day based on electricity demand. For example, the price is higher during peak load conditions and lower during load valleys. Several studies have considered the ToU price for PEV charging to control their load [36], [37], [38], [39], [40]. To encourage customers to charge their vehicles during the load valleys and minimize peak loads, the authors in [41] analyzed the charging impact on load cycle and designed an innovative real-time ToU pricing system.

In this subsection, we propose the dynamic pricing model for PEV charging and discharging correlated with the ToU price in the power market. Fig. 6 shows the energy and money exchange model for the proposed dynamic pricing system. The microgrid imports electrical power from the utility provider under the wholesale sell-in ToU price marked as  $\varphi_{ToU}$  and exports to the power market at the system margin price (SMP) represented by  $\varphi_{SMP}$ . Both  $\varphi_{ToU}$  and  $\varphi_{SMP}$

are time-varying prices and given by the distribution system operator (DSO).

In this paper, we define  $\varphi_{ch}$  and  $\varphi_{disch}$  as the charging and discharging prices of PEVs in the microgrid, respectively. PEV owners will charge  $\varphi_{ch}$  for their PEV charging to the microgrid operator and receive  $\varphi_{disch}$  from the operator when their PEVs discharge to support the microgrid operation, such as peak load mitigation and so on. The proposed electricity prices are determined dynamically depending on the operation modes of the microgrid, such as normal operation, peak-demand, and high-PV-generation modes.

The PEV charging and discharging prices are determined by the loading conditions of the microgrid, which can be classified by the net load defined as

$$P_{NL}^i = P_L^i - P_{PV}^i \quad (20)$$

where  $P_{NL}^i$  is the net load at the  $i$ -th interval, and  $P_L^i$  and  $P_{PV}^i$  are the load consumption and PV power generation at the  $i$ -th interval, respectively.

In the normal operation mode, when the net load power is under the critical maximum power import ( $P_{cri}$ ), the PEVs can be in the idle or charging mode, and the PEV charging price is set to the ToU price ( $\varphi_{ch}^i = \varphi_{ToU}^i$ ). PEVs are not encouraged to discharge during normal operation. However, if there is an emergency for discharging, the PEV discharging price is the same as the ToU price at that interval ( $\varphi_{disch}^i = \varphi_{ToU}^i$ ).

In the peak-demand period, when the net load is much higher than the critical power import, the PEVs are encouraged to discharge their batteries to reduce the peak load below the critical power ( $P_{cri}$ ). The incentive ( $\gamma$ ) is added to the discharge price, whereas charging actions are restricted in this period by addition of a high penalty ( $\beta$ ). The proposed charging and discharging prices are determined as follows:

$$\varphi_{ch}^i = \varphi_{ToU}^i + \beta \quad (21)$$

$$\varphi_{disch}^i = \varphi_{ToU}^i + \gamma \quad (22)$$

Here,  $\beta$  and  $\gamma$  are the penalty charge and incentive for PEV charging and discharging, respectively. These are determined monthly by the system operator based on data from the previous month. The penalty is normally determined as the peak-demand charging rate according to the PEV charging tariff defined by the utility provider. The incentive for PEV discharging is to encourage discharge of the PEV battery to enable reduction in peak-demand charges. For example, it can be determined as half of  $\beta$ .

In high-PV power generation, the microgrid operator proposes the PEV charging price based on the SMP and ToU prices. The microgrid operator will sell their excess power to the power market at the SMP rate, while simultaneously offering a competitive charging price to incentivize PEVs to charge their batteries, as depicted in equation (23). However, discharging actions are not encouraged in this mode. The proposed charging and discharging prices are



determined as follows:

$$\varphi_{ch}^i = \min \left( \varphi_{SMP}^i, \frac{\varphi_{SMP}^i + \varphi_{ToU}^i}{2} \right) \quad (23)$$

$$\varphi_{disch}^i = \min \left( \varphi_{SMP}^i, \varphi_{ToU}^i \right) \quad (24)$$

### III. SIMULATION RESULTS AND DISCUSSION

#### A. CASE STUDIES

To verify the performance of the proposed algorithm, we implemented a simulation model of a microgrid system as shown in Fig. 1. PVs are installed in the microgrid, and the PV output power is forecast based on the RNN-LSTM algorithm [20], [21]. In this simulation, we assume that the minimum peak demand (critical power) in the previous 12 months is 150 kW. Therefore, the MG-EMS tries to maintain the peak demand around the critical power and charge the PEV during high PV power generation.

There are four PEV charging stations with V2G capability installed in the microgrid. The charging stations limit the maximum charging powers to 9.6 kW, 13.2 kW, 19.6 kW, and 13.2 kW. Assuming that various PEV models with different battery sizes, such as 25 kWh, 32 kWh, 35 kWh, and 42 kWh, arrive at the charging station for charging and discharging, the details of the PEVs for the simulations are presented in Table 1. The simulations are implemented using MATLAB 2019a, and the MILP optimization problem is solved using the CPLEX/MATLAB optimizer toolbox.

Table 2 shows the ToU electricity prices for load consumption and PEV charging power. The simulations are applied for the summer season. The season categories are classified in Table 3 as off-peak, mid-peak, and on-peak periods.

Fig. 7 presents the forecast load consumption and solar power generation for the simulation cases. The peak demand occurs around 19:00 PM. PV solar power is maximum from 12:00 PM to 13:00 PM. Fig. 8 indicates the SMP price applicable to energy selling to the power market; these ToU and SMP prices were obtained from a utility company as of 05 May 2021

In the conventional approach, for charging PEVs, ToU pricing is utilized and no discharging function is integrated. Conversely, the proposed dynamic pricing scheme allows efficient calculation of costs associated with charging and discharging PEVs because the proposed approach allows both charging and discharging mechanisms for PEVs. For surplus energy export, SMP is employed for both conventional and proposed approach. Fig. 8(a) depicts the ToU prices at various time periods and the 24-hour SMP as on May 5, 2021, as provided by the utility company. Fig. 8(b) illustrates the dynamic pricing for PEV charging and discharging according to the proposed dynamic pricing algorithm. It is evident from the figure that the charging price at peak power generation, i.e., at time step 14, using our proposed algorithm is significantly lower than the ToU price, reaching a value of approximately 157 KRW/kWh compared to 232.3 KRW/kWh when using the ToU pricing. Additionally,

TABLE 2. Initial information of the EVs for the simulations.

PEV No.	EVCS No.	Arr. Time	Dept. Time	PEV Cap (kWh)	Init. SoC (%)	Dept. SoC (%)
1	#1	02 AM	08 AM	32	20	80
2	#3	02 AM	12 PM	35	20	90
3	#2	03 AM	13 PM	42	20	90
4	#4	04 AM	16 PM	35	20	85
5	#1	11 AM	17 PM	25	20	85
6	#3	14 PM	21 PM	35	20	85
7	#2	15 PM	00 AM	35	20	90
8	#4	18 PM	00 AM	25	20	80
9	#1	19 PM	00 AM	32	20	75

TABLE 3. Time-of-use (TOU) electricity prices for power import.

Time period	Energy charge (KRW/kWh) <sup>(1)</sup>		
	Summer	Spring/Fall	Winter
Off-peak	57.6	58.7	80.7
Mid-peak	145.3	70.5	128.2
On-peak	232.3	75.4	190.6

(1) KRW is Korean Won, which is the official currency of South Korea, 1 US Dollar (USD) is about 1,113 KRW as of Oct 2021.

TABLE 4. Season and time period classification.

Classification	Summer, Spring and the Fall (**)	Winter (*)
Off-peak	23:00-09:00	23:00-09:00
	09:00-10:00	09:00-10:00
Mid-peak	12:00-13:00	12:00-17:00
	17:00-23:00	20:00-22:00
On-peak	10:00-12:00	10:00-12:00
	13:00-17:00	17:00-20:00 22:00-23:00

(\*\*) Summer: June–August; Spring: March–May; Fall: September and October; (\*) Winter: November–February.

during peak load periods, the high penalty costs associated with PEV charging are significantly higher, as indicated by the graph in Fig. 8(b), which shows charging and discharging prices up to a maximum of 2725.3 and 1435.3 KRW/kWh, respectively. Owing to the significant differences in charging/discharging prices between the off-peak and on-peak periods, we utilize a logarithmic scale on the y-axis to display all values in the horizon in Fig. 8(b).

#### B. RESULT SIMULATIONS AND COMPARISON WITH THE CONVENTIONAL METHOD

A case study was performed with the aim of evaluating the efficacy of the proposed optimal control strategy utilizing the ARH framework. To gauge the performance of this strategy, it was compared with the conventional charging operation, in which PEVs are charged as soon as they are connected to the system without taking into account the possibility of discharging them. It is worth noting that the conventional method does not consider the time-varying nature of

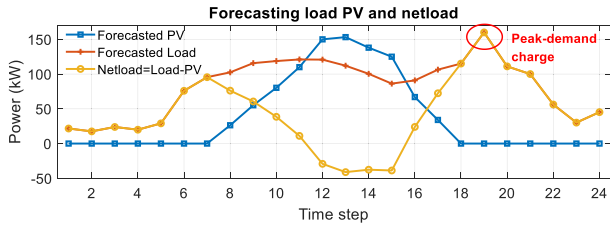


FIGURE 7. Load and PV power generation forecasting.

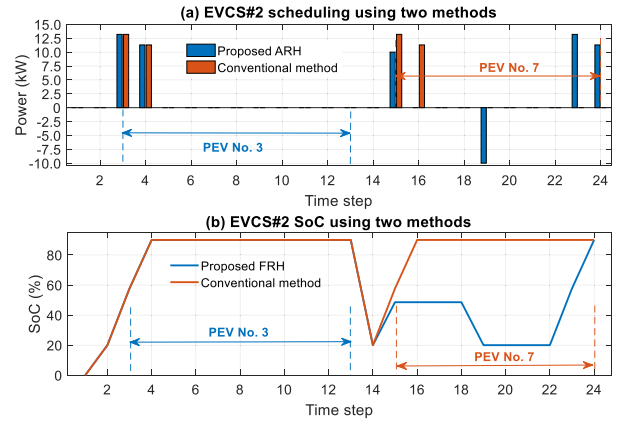


FIGURE 10. EV charging/discharging scheduling at EVCS#2 using two methods.

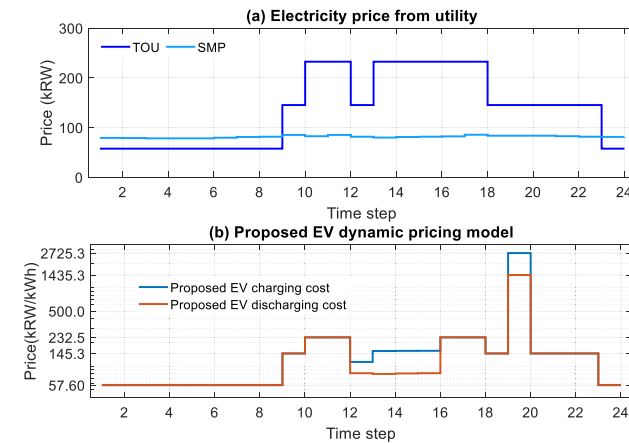


FIGURE 8. Dynamic pricing model for EV charging/discharging.

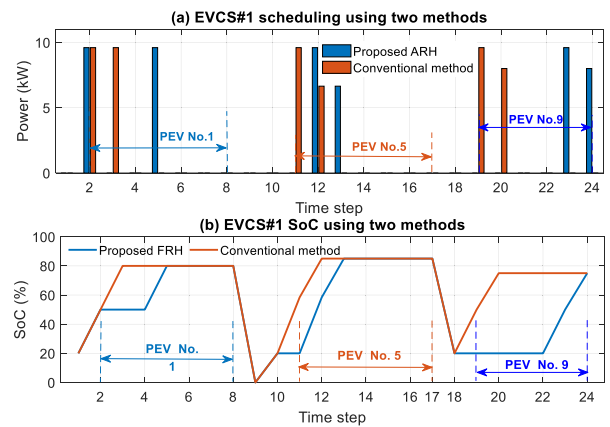


FIGURE 9. EV charging/discharging scheduling at EVCS#1 using two methods.

electricity prices or potential cost savings that can be realized by strategically shifting the times at which PEVs are charged and discharged. Ultimately, the results of the case study demonstrate that the proposed ARH framework outperformed the conventional method in terms of overall effectiveness.

The results of scheduling comparisons between the conventional and proposed methods are presented in Figs. 9(a), 10(a), 11(a), and 12(a), which demonstrate the performances of the two approaches over the course of a single day consisting of 24-time steps. In the proposed approach, the MG-EMS continuously updates its information as new PEVs connect to the system and subsequently runs an optimization process

to minimize the total operating cost while optimizing the total PEV charging power. As depicted in Fig. 10(a), there are two PEVs connected to EVCS#2 over the course of the 24-hour period. These PEVs are scheduled to charge during periods of low electricity prices and discharge during the peak-demand periods so as to reduce the overall peak power demand on the system. For example, the second PEV (PEV No.7) is shown to be plugged-in at 15:00 and leaving at midnight, during which time it charges its battery in three-time steps with low electricity prices at 15:00, 23:00, and 24:00 while discharging its battery during the peak-demand period at 19:00 to reduce the peak power from 160 kW to 150 kW, as shown in Fig. 13(b). This reduction in the peak power demand allows the PEV owner to receive an incentive payment that compensates their electricity charging bill as they leave, as shown in Fig. 14.

The SoCs of the PEVs at various EVCS are depicted in Fig. 9(b) through Fig. 12(b). At EVCS#1, there are three PEVs that arrive to charge their batteries. The first of these arrives at 2:00 AM and leaves at 8:00 AM, with an expected departure SoC of 80% for the next trip. As shown in Fig. 9(a), this PEV charges its battery in two-time steps during the low peak periods to reach the desired departure. At EVCS#2, two PEVs are shown to be plugged-in and charging their batteries. The second of these arrives at 15:00 PM and immediately begins charging its battery with a power of 10 kW at the mid-peak electricity price and discharges for the peak-demand period at 19:00 PM. As a result, the SoC of this PEV increases from 20% to 45% by the end of 15:00 PM and decreases to 20% at 19:00 PM. Afterward, the PEV battery is charged at 23:00 PM and 24:00 AM during the off-peak period to fill its SoC to 90%.

Fig. 13 presents a comparison of the exported/imported power to/from the grid for the two methods. Fig. 13(a) illustrates the result of the conventional method, which demonstrates that PEV charging increases peak demand as shown in the red circle, resulting in additional costs for the microgrid operator. As shown in the figure, the charging of

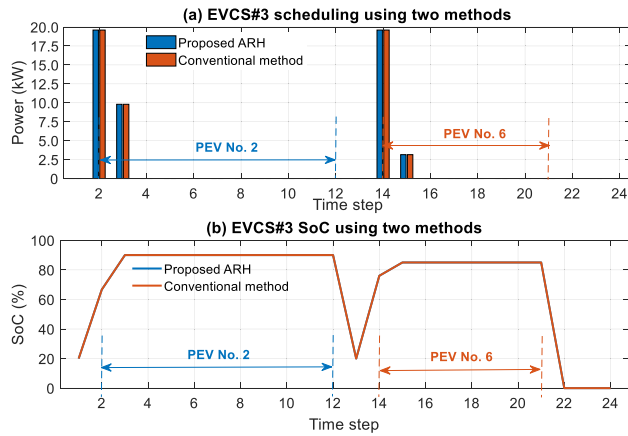


FIGURE 11. PEV charging/discharging scheduling at EVCS#3 using two methods.

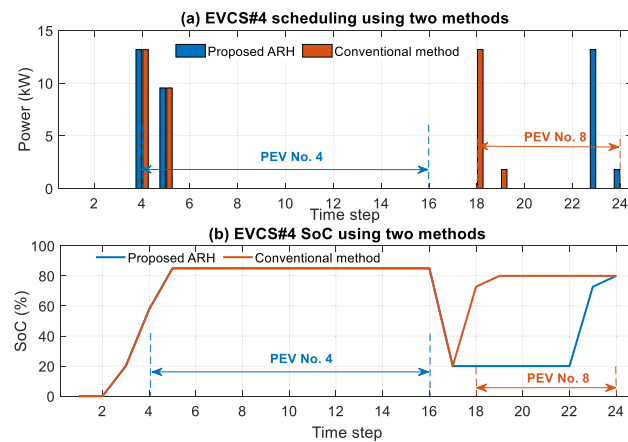


FIGURE 12. PEV charging/discharging scheduling at EVCS#3 using two methods.

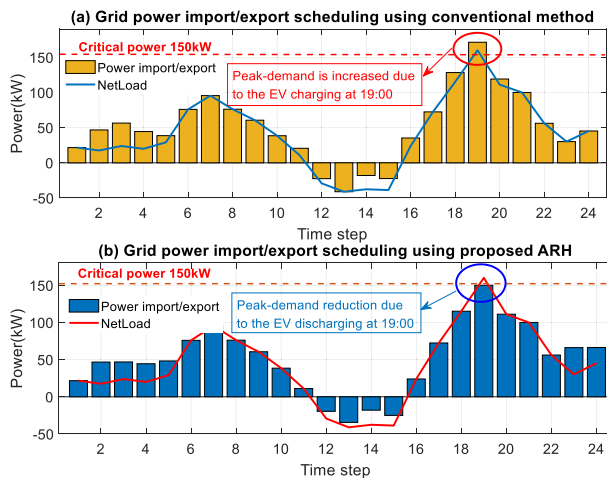


FIGURE 13. Comparison of power imported/exported from/to the utility distribution grid using two methods.

the PEVs at various times, such as 2:00, 3:00, 4:00, 5:00, 11:00, 12:00, 14:00, 15:00, 16:00, 18:00, 19:00, and 20:00, causes an increase in the net load, leading to a peak demand

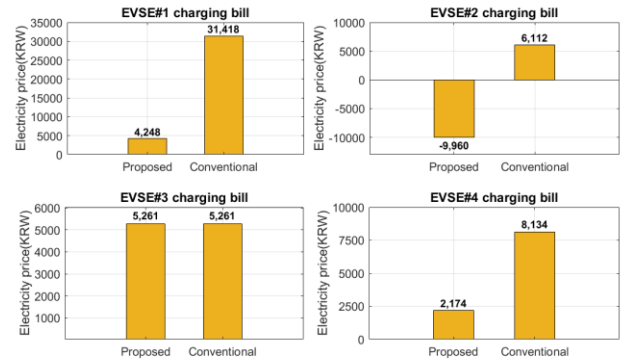


FIGURE 14. PEV charging payment comparisons between two methods.

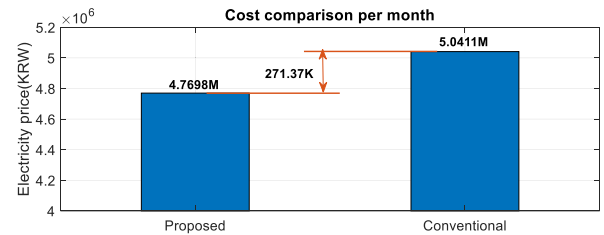


FIGURE 15. Comparison of total operating cost of MG between two methods.

of 171.2 kW at 19:00 PM which is higher than the critical power threshold of 150 kW represented by the horizontal dashed-line. On the other hand, Fig. 13(b) shows the imported/exported power using the proposed method, which effectively reduces peak demand through PEV scheduling, thereby avoiding peak-demand charges. Similar to the conventional method, charging of the PEVs causes an increase in the net load during some periods; however, by strategically scheduling the PEVs to allow compensation of the peak demand through PEV discharging, the proposed approach is able to reduce the peak demand from 160 kW to the expected critical power of 150 kW at 19:00. This demonstrates the effectiveness of the proposed method in mitigating the negative impacts of PEV charging on the overall power demand of the system.

Fig. 14 provides a comparison of the PEV users' satisfaction based on the descriptions of their charging bills. It is readily apparent that the total charging descriptions for the four EVCS are reduced through the use of the proposed control method. At EVCS#2, the PEV owners are able to receive incentive payments for discharging power, which is used to compensate for the peak demand. This is reflected in the reduced charging costs for these users. Fig. 15 presents a comparison of the total operating cost of the microgrid over the course of a month, highlighting the cost savings that can be achieved through the use of the proposed method. The value of these savings is shown to be 271,370 KRW per month, demonstrating the significant benefits of the proposed approach for both PEV users and the microgrid operator.

#### IV. CONCLUSION

In this study, we utilize PV power generation capabilities and PEVs present in a microgrid to optimize the overall operating cost and charging expenses for the PEVs. To accomplish this, we formulated an optimal control strategy using MILP with an ARH. To ensure that all of the participating PEVs are taken into consideration in the optimization process, we proposed the concept of the ARH that allows dynamic pricing modifications of the horizon at each time step.

In addition, to minimize the operating cost and charging expenses for the PEVs, we suggest implementation of a dynamic pricing model for both charging and discharging based on the operational mode of the microgrid. This pricing model allows all relevant information to be updated at regular intervals to facilitate optimization.

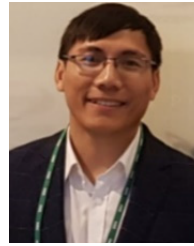
To further enhance the efficiency of our approach, we incorporated an advance forecasting algorithm based on the LSTM-RNN to predict the local load demand and output power of the PV plant.

We conducted a case study in which the proposed method was compared with the conventional method. The simulation results obtained through this comparison provide numerical evidence that our proposed method is more cost-effective than the conventional approach in terms of both operating costs and charging expenses for PEVs. These findings demonstrate the superiority of our proposed framework and its potential to significantly reduce costs while improving the efficiency in of the microgrid system.

#### REFERENCES

- [1] M. E. Khodayar, M. Barati, and M. Shahidehpour, "Integration of high reliability distribution system in microgrid operation," *IEEE Trans. Smart Grid*, vol. 3, no. 4, pp. 1997–2006, Dec. 2012.
- [2] D. Zhang, N. Shah, and L. G. Papageorgiou, "Efficient energy consumption and operation management in a smart building with microgrid," *Energy Convers. Manage.*, vol. 74, pp. 209–222, Oct. 2013.
- [3] F. Katiraei and M. R. Iravani, "Power management strategies for a microgrid with multiple distributed generation units," *IEEE Trans. Power Syst.*, vol. 21, no. 4, pp. 1821–1831, Nov. 2006.
- [4] M. A. Sofla and G. B. Gharehpetian, "Dynamic performance enhancement of microgrids by advanced sliding mode controller," *Int. J. Electr. Power Energy Syst.*, vol. 33, no. 1, pp. 1–7, Jan. 2011.
- [5] L. Shi, Y. Luo, and G. Y. Tu, "Bidding strategy of microgrid with consideration of uncertainty for participating in power market," *Int. J. Electr. Power Energy Syst.*, vol. 59, pp. 1–13, Jul. 2014.
- [6] J. J. Justo, F. Mwasilu, J. Lee, and J.-W. Jung, "AC-microgrids versus DC-microgrids with distributed energy resources: A review," *Renew. Sustain. Energy Rev.*, vol. 24, pp. 387–405, Aug. 2013.
- [7] K. Zhang, L. Xu, M. Ouyang, H. Wang, L. Lu, J. Li, and Z. Li, "Optimal decentralized valley-filling charging strategy for electric vehicles," *Energy Convers. Manage.*, vol. 78, pp. 537–550, Feb. 2014.
- [8] M. A. Hannan, F. A. Azidin, and A. Mohamed, "Multi-sources model and control algorithm of an energy management system for light electric vehicles," *Energy Convers. Manage.*, vol. 62, pp. 123–130, Oct. 2012.
- [9] Q. Zhang, K. N. Ishihara, B. C. McLellan, and T. Tezuka, "Scenario analysis on future electricity supply and demand in Japan," *Energy*, vol. 38, no. 1, pp. 376–385, Feb. 2012.
- [10] A. Zakariazadeh, S. Jadid, and P. Siano, "Stochastic multi-objective operational planning of smart distribution systems considering demand response programs," *Electr. Power Syst. Res.*, vol. 111, pp. 156–168, Jun. 2014.
- [11] B. Soares M. C. Borba, A. Szklo, and R. Schaeffer, "Plug-in hybrid electric vehicles as a way to maximize the integration of variable renewable energy in power systems: The case of wind generation in northeastern Brazil," *Energy*, vol. 37, no. 1, pp. 469–481, Jan. 2012.
- [12] A. Di Giorgio, F. Liberati, and S. Canale, "Electric vehicles charging control in a smart grid: A model predictive control approach," *Control Eng. Pract.*, vol. 22, pp. 147–162, Jan. 2014.
- [13] L. Igualada, C. Corchero, M. Cruz-Zambrano, and F. Heredia, "Optimal energy management for a residential microgrid including a vehicle-to-grid system," *IEEE Trans. Smart Grid*, vol. 5, no. 4, pp. 2163–2172, Jul. 2014.
- [14] Y. Guo, J. Xiong, S. Xu, and W. Su, "Two-stage economic operation of microgrid-like electric vehicle parking deck," *IEEE Trans. Smart Grid*, vol. 7, no. 3, pp. 1703–1712, May 2016.
- [15] W. Su, J. Wang, K. Zhang, and A. Q. Huang, "Model predictive control-based power dispatch for distribution system considering plug-in electric vehicle uncertainty," *Electr. Power Syst. Res.*, vol. 106, pp. 29–35, Jan. 2014.
- [16] M. van der Kam and W. van Sark, "Smart charging of electric vehicles with photovoltaic power and vehicle-to-grid technology in a microgrid; a case study," *Appl. Energy*, vol. 152, pp. 20–30, Aug. 2015.
- [17] Z. Ma, D. S. Callaway, and I. A. Hiskens, "Decentralized charging control of large populations of plug-in electric vehicles," *IEEE Trans. Control Syst. Technol.*, vol. 21, no. 1, pp. 67–78, Jan. 2013.
- [18] M. Shahbazitabar and H. Abdi, "A novel priority-based stochastic unit commitment considering renewable energy sources and parking lot cooperation," *Energy*, vol. 161, pp. 308–324, Oct. 2018.
- [19] X. Tan, Q. Li, and H. Wang, "Advances and trends of energy storage technology in microgrid," *Int. J. Electr. Power Energy Syst.*, vol. 44, no. 1, pp. 179–191, Jan. 2013.
- [20] S. Hussain, R. R. Irshad, F. Pallonetto, Q. Jan, S. Shukla, S. Thakur, J. G. Breslin, M. Marzband, Y.-S. Kim, M. A. Rathore, and H. El-Sayed, "Enhancing the efficiency of electric vehicles charging stations based on novel fuzzy integer linear programming," *IEEE Trans. Intell. Transp. Syst.*, vol. 24, no. 9, pp. 9150–9164, Sep. 2023, doi: 10.1109/TITS.2023.3274608.
- [21] S. Hussain, Y.-S. Kim, S. Thakur, and J. G. Breslin, "Optimization of waiting time for electric vehicles using a fuzzy inference system," *IEEE Trans. Intell. Transp. Syst.*, vol. 23, no. 9, pp. 15396–15407, Sep. 2022, doi: 10.1109/TITS.2022.3140461.
- [22] J. Silvente, G. M. Kopanos, E. N. Pistikopoulos, and A. Espuña, "A rolling horizon optimization framework for the simultaneous energy supply and demand planning in microgrids," *Appl. Energy*, vol. 155, pp. 485–501, Oct. 2015, doi: 10.1016/j.apenergy.2015.05.090.
- [23] Z. Li, C. Zang, P. Zeng, and H. Yu, "Combined two-stage stochastic programming and receding horizon control strategy for microgrid energy management considering uncertainty," *Energies*, vol. 9, no. 7, p. 499, Jun. 2016, doi: 10.3390/en9070499.
- [24] E. Srilakshmi and S. P. Singh, "Energy regulation of EV using MILP for optimal operation of incentive based prosumer microgrid with uncertainty modelling," *Int. J. Electr. Power Energy Syst.*, vol. 134, Jan. 2022, Art. no. 107353, doi: 10.1016/j.ijepes.2021.107353.
- [25] J. Hu, H. Zhou, Y. Li, P. Hou, and G. Yang, "Multi-time scale energy management strategy of aggregator characterized by photovoltaic generation and electric vehicles," *J. Mod. Power Syst. Clean Energy*, vol. 8, no. 4, pp. 727–736, Jul. 2020, doi: 10.35833/MPCE.2019.000464.
- [26] M. Husein and I.-Y. Chung, "Day-ahead solar irradiance forecasting for microgrids using a long short-term memory recurrent neural network: A deep learning approach," *Energies*, vol. 12, no. 10, p. 1856, May 2019, doi: 10.3390/en12101856.
- [27] R. Zafar, B. H. Vu, M. Husein, and I.-Y. Chung, "Day-ahead solar irradiance forecasting using hybrid recurrent neural network with weather classification for power system scheduling," *Appl. Sci.*, vol. 11, no. 15, p. 6738, Jul. 2021, doi: 10.3390/app11156738.
- [28] E. Amicarelli, T. Q. Tran, and S. Bacha, "Optimization algorithm for microgrids day-ahead scheduling and aggregator proposal," in *Proc. IEEE Int. Conf. Environ. Electr. Eng. IEEE Ind. Commercial Power Syst. Eur.*, Jun. 2017, pp. 1–6, doi: 10.1109/EEEIC.2017.7977487.
- [29] M. Vosoogh, M. Rashidinejad, A. Abdollahi, and M. Ghaseminezhad, "An intelligent day ahead energy management framework for networked microgrids considering high penetration of electric vehicles," *IEEE Trans. Ind. Informat.*, vol. 17, no. 1, pp. 667–677, Jan. 2021, doi: 10.1109/TII.2020.2977989.

- [30] P.-H. Trinh and I.-Y. Chung, "Optimal control strategy for distributed energy resources in a DC microgrid for energy cost reduction and voltage regulation," *Energies*, vol. 14, no. 4, p. 992, Feb. 2021, doi: [10.3390/en14040992](https://doi.org/10.3390/en14040992).
- [31] X. Zhaoxia, L. Hui, Z. Tianli, and L. Huaimin, "Day-ahead optimal scheduling strategy of microgrid with EVs charging station," in *Proc. IEEE 10th Int. Symp. Power Electron. for Distrib. Gener. Syst. (PEDG)*, Jun. 2019, pp. 774–780, doi: [10.1109/PEDG.2019.8807656](https://doi.org/10.1109/PEDG.2019.8807656).
- [32] J. Su, T. T. Lie, and R. Zamora, "A rolling horizon scheduling of aggregated electric vehicles charging under the electricity exchange market," *Appl. Energy*, vol. 275, Oct. 2020, Art. no. 115406, doi: [10.1016/j.apenergy.2020.115406](https://doi.org/10.1016/j.apenergy.2020.115406).
- [33] Y. Cao, S. Tang, C. Li, P. Zhang, Y. Tan, Z. Zhang, and J. Li, "An optimized EV charging model considering TOU price and SOC curve," *IEEE Trans. Smart Grid*, vol. 3, no. 1, pp. 388–393, Mar. 2012.
- [34] C. Li, S. Tang, Y. Cao, Y. Xu, Y. Li, J. Li, and R. Zhang, "A new stepwise power tariff model and its application for residential consumers in regulated electricity markets," *IEEE Trans. Power Syst.*, vol. 28, no. 1, pp. 300–308, Feb. 2013.
- [35] D. S. Kirschen, G. Strbac, P. Cumperayot, and D. de Paiva Mendes, "Factoring the elasticity of demand in electricity prices," *IEEE Trans. Power Syst.*, vol. 15, no. 2, pp. 612–617, May 2000.
- [36] D. Said, S. Cherkaoui, and L. Khoukhi, "Advanced scheduling protocol for electric vehicle home charging with time-of-use pricing," in *Proc. IEEE Int. Conf. Commun. (ICC)*, Jun. 2013, pp. 6272–6276.
- [37] B. Geng, J. K. Mills, and D. Sun, "Coordinated charging control of plug-in electric vehicles at a distribution transformer level using the vTOU-DP approach," in *Proc. IEEE Vehicle Power Propuls. Conf.*, Oct. 2012, pp. 1469–1474.
- [38] M. Hemphill, "Electricity distribution system planning for an increasing penetration of plug-in electric vehicles in new south Wales," in *Proc. 22nd Australas. Universities Power Eng. Conf. (AUPEC)*, Sep. 2012, pp. 1–6.
- [39] M. Mallette and G. Venkataramanan, "Financial incentives to encourage demand response participation by plug-in hybrid electric vehicle owners," in *Proc. IEEE Energy Convers. Congr. Expo.*, Sep. 2010, pp. 4278–4284.
- [40] Y. Gao, C. Wang, Z. Wang, and H. Liang, "Research on time-of-use price applying to electric vehicles charging," in *Proc. IEEE Innov. Smart Grid Technol. Asia*, Mar. 2012, pp. 1–6.
- [41] Q. Yan, I. Manickam, M. Kezunovic, and L. Xie, "A multi-tiered real-time pricing algorithm for electric vehicle charging stations," in *Proc. IEEE Transp. Electrification Conf. Expo (ITEC)*, Jun. 2014, pp. 1–6, doi: [10.1109/ITEC.2014.6861790](https://doi.org/10.1109/ITEC.2014.6861790).
- [42] M. S. Mastoi, S. Zhuang, H. M. Munir, M. Haris, M. Hassan, M. Usman, S. S. H. Bukhari, and J.-S. Ro, "An in-depth analysis of electric vehicle charging station infrastructure, policy implications, and future trends," *Energy Rep.*, vol. 8, pp. 11504–11529, Nov. 2022, doi: [10.1016/j.egyr.2022.09.011](https://doi.org/10.1016/j.egyr.2022.09.011).
- [43] *Electric Vehicle Database*. Accessed: May 10, 2021. [Online]. Available: <https://ev-database.org/>



**PHI-HAI TRINH** (Student Member, IEEE) received the B.S. degree in electrical engineering from the Ho Chi Minh City University of Technology, Vietnam, in 2012, and the Ph.D. degree in electronics engineering from Kookmin University, Seoul, South Korea, in 2020.

He has been a Research Professor with Kookmin University, since 2023. His current research interests include optimal control and operation of microgrids, distributed energy resource management systems, model predictive control for energy systems, and voltage control for distribution systems.



**REHMAN ZAFAR** (Student Member, IEEE) received the B.S. degree in electrical engineering from COMSATS University Islamabad, Pakistan, in 2015. He is currently pursuing the Ph.D. degree in electronics engineering with Kookmin University, Seoul, South Korea.

He has been a Graduate Researcher with Kookmin University, since 2017. His research interests include AI for power system applications, renewable integration to power grids, and power system control and operation.



**IL-YOP CHUNG** (Member, IEEE) received the B.S., M.S., and Ph.D. degrees in electrical engineering from Seoul National University, Seoul, South Korea, in 1999, 2001, and 2005, respectively.

He was a Postdoctoral Associate with Virginia Tech, Blacksburg, VA, USA, from 2005 to 2007. From 2007 to 2010, he was with the Center for Advanced Power Systems, Florida State University, Tallahassee, FL, USA, as an Assistant Scholar Scientist. He is currently a Full Professor with the School of Electrical Engineering, Kookmin University, Seoul. His research interests include power system control and operation, renewable energy integration to power grids, remote microgrids with renewable energy, and shipboard power systems.

• • •